IOSR Journal of Applied Physics (IOSR-JAP)
e-ISSN: 2278-4861.Volume 7, Issue 2 Ver. III (Mar. - Apr. 2015), PP 51-61
www.iosrjournals.org

Early Stage of Target Fragmentation Induced by Light Nuclei at E_{LAB} ~ 2A GEV

N. Rashed
Physics Department, Faculty of Science, Fayoum University, Fayoum, Egypt.

Abstract: *Forward–backward grey particle productions following 2.1A GeV ^{4}He and 2.2A GeV ^{7}Li interactions with emulsion nuclei are investigated. The grey particle multiplicity characteristics are found to be dependent only on the target size where the projectile size and energy are not effective. The validity of the nuclear limiting fragmentation hypothesis is examined with respect to the projectile size and energy. The characteristic shape of the forward and backward emitted grey particle multiplicity distributions is decay curves. These distributions are approximated by an exponential decay law. The fit parameters characterizing this law decrease with the target size. The production probabilities and the average multiplicities increase linearly with the target size. The defined asymmetry parameter and anisotropy ratio between the forward and backward production systems, ~ 0.5 and 3 respectively, are constant irrespective of the system size. According to the kinematics of the target rest frame in the framework of the fireball model, the recoiled target nucleon is suggested to be emitted in the forward hemisphere as a result of the binary nucleon–nucleon collisions or intranuclear cascading. The results show that the forward emitted grey particle is three times the backward emitted one. Hence, the main grey particle production source is the intranuclear cascading. Although the emission in the backward hemisphere, beyond the kinematic limits, is suggested to result from a different source, however a scaling feature is observed between the multiplicity characteristics of the two emission systems. This scaling is assessed. On the basis of the nuclear limiting fragmentation validity and the assessed scaling between the two emission systems in the 4–π space, the grey particle multiplicity characteristics can be determined in a universal law.*

Keywords: *^{4}He and ^{7}Li as Light Projectiles / Grey Particle Multiplicity in Terms of System Size and Emission Direction / Nuclear Limiting Fragmentation in A Few A GeV Energy Region / Scaling Indications between The Forward and Backward Emission Systems.*

I. Introduction

In high–energy nuclear collisions, multiple sources of particle production are needed. The fragmentation cross–section can be limited w. r. t. the energy beyond E_{lab} ~ 1A GeV. This energy value can be considered the onset of the nuclear limiting fragmentation, NLF, region. The NLF hypothesis is valid in the few A GeV region, as Dubna energy [1], SPS [2], RHIC [3], and LHC [4] energies. In this regime, the target nucleus is fragmented into nucleons and emitted in the 4–π space within a limited multiplicity at a certain impact parameter, irrespective of the energy or projectile size.

In the framework of the statistical thermodynamical model Heckman et al [5] modify the Maxwell–Boltzmann distribution by which the emission system of the slow target fragment can be predicted. Accordingly, this emission system is thermalized. In the light of this model, the emission system of the fast target fragment can be predicted [6], where it is also suggested to be thermalized. Abdelsalam et al [7] predict the temperature of these two emission systems as near as 6 and 60 MeV, respectively. Therefore, the target fragmentation system emits particles not only in one stage of time but in two stages. They are the fast and slow target nucleons which are emitted in the hotter early and later stages, respectively. In the collision system, a quasi–equilibrated region, called fireball, can be formed in the overlapping between the projectile and the target nuclei [8]. Inside the overlapping region, the projectile and target nucleons are participated while those outside are the spectators. At Bevalac energies, (E_{lab} ~ 0.1A up to 2A GeV), the fireball temperature ranges from 30 up to 125 MeV [9]. Therefore the early stage of the target fragmentation has to deal with the emission from the hot participant region, where the fireball is formed. In the later stage, the emission seems to associate with the target spectator part.

In the photographic nuclear emulsion the fast and slow target protons can be attributed to the grey and black particles tracks, respectively [10, 11]. The grey particle is expected to be emitted through the binary nucleon–nucleon, NN, collisions and/or intranuclear cascading [12–15]. In the framework of the modified cascade evaporation model, MCEM, [16] the intranuclear cascading can not only be by the primary nucleon, but also by the created parton during the formation time of the final state hadron. The struck nucleon recoils and may be emitted where the grey particle can be observed. During the cascading, the spectator part of the target nucleus is highly excited. After a long time w. r. t. the hadron formation time, the spectator part is thermalized by losing its excitation energy through an evaporation. The slow fragments, including the black particles, are

emitted in this evaporation process. According to this elucidation, the kinematics of the collision system imply that the particle must be emitted in the forward hemisphere, FHS, within $\theta_{lab} < 90^{\circ}$. However, another emission system can be observed beyond the kinematic limits at $\theta_{lab} \geq 90^{\circ}$ in the backward hemisphere, BHS. Harris [17] assumes two possible mechanisms through which this emission can occur. The first is a pion production followed by its absorption on two target nucleons. Then they are emitted back–to–back. The second is a production of Δ^{++} which is observed by one target nucleon through the mode, $\Delta N \rightarrow NN$. The outgoing nucleons are emitted back–to–back.

Actually, the fixed target experiments are consideredguidelines in simulating and equipping the systems through which the nuclear fragmentation is applied practically. Since the fragmentation system is limited w. r. t. the energy, this type of experiments does not need a big amount of energy as that used with the collider ones. In this experiment some characteristics, associated with the early stage of the target fragmentation, are overviewed using 2.1A GeV ^{4}He and 2.2A GeV ^{7}Li interactions with emulsion nuclei. The grey particle multiplicity characteristics are determined in terms of the target size and emission direction. The present energies are nearly constant, E_{lab} ~ 2A GeV. Here, the NLF validity can be examined w. r. t. the size of the present light projectiles in the few A GeVregion. The used data are from the data bank of Mohamed El–Nadi high energy lab, faculty of science, Cairo university, Egypt.

II. Experimental Details

In this experiment the NIKFI–BR2 nuclear emulsion stacks are irradiated by 2.1A GeV ^{4}He and 2.2A GeV ^{7}Li beams at the Synchrophasotron, JINR, Dubna, Russia. Each pellicle of the stack has a dimensions 10 cm × 20 cm × 0.06 cm. The chemical composition of this emulsion type is listed in Table (1). The density, ρ, of the emulsion nuclei is listed also in Table (1).

Table (1): The chemical composition of the NIKFI–BR2 emulsion.

Element	^{1}H	^{12}C	^{14}N	^{16}O	^{80}Br	^{108}Ag
ρ atoms/cm^3	3.150	1.410	0.395	0.956	1.028	1.028

The experimental technique, methods, and equipments are the same as those obeyed in Ref. [18]. The total scanned lengths, L, of the present beams, the associated number of inelastic interactions, N, and the corresponding average mean free path, λ, are listed in Table (2). The mean free path is determined as; $\lambda = L/N$.

Table (2): The present beams interactions data.

Projectile	L m	N events	λ cm
^{4}He	416.5	2006	20.16±0.44
^{7}Li	153.5	1003	15.30±0.48

The produced charged particles per event can be identified in the photographic nuclear emulsion according to their ionization characteristics [10, 11]. They are classified into the below categories.

- The shower particles are mainly pions having K. E > 70 MeV and about 10% charged hadrons with K. E > 400 MeV. Their multiplicity is denoted n_s. The multiplicity of the forward and backward emitted shower particles are denoted n_s^f and n_s^b, respectively.
- The grey particles are mainly of knocked out target protons with 26 < K. E < 400 MeV. They have a little admixture of mesons. Their multiplicity is denoted as N_g. The multiplicity of the forward and backward emitted grey particles are denoted N_g^f and N_g^b, respectively.
- The black particles are evaporated target protons with k. E < 26 MeV. Their multiplicity is denoted as N_b.
- The grey and black particles amount the group of heavily ionizing particles, denoted $N_h = N_g + N_b$.
- The projectile fragments are nuclear isotopes having $Z \geq 1$. They fly with the same speed of the projectile nucleus and are emitted in the forward narrow cone within $\theta_{lab} \leq 3^{\circ}$.

III. Results And Discussion

Mentioned above, in Table (1), that the nuclear emulsion consists of different nuclei with the displayed densities. In this work the target size is accounted by the statistical events associated with H, CNO (the light target nuclei), Em (the nuclear emulsion as a whole), and AgBr (the heavy target nuclei). The effective mass numbers of these targets are 1, 14, 70, and 94, respectively. Herein after, any data belonging to 2.1A GeV ^{4}He and 2.2A GeV ^{7}Li are presented diagrammatically by open and closed squares, respectively. In same respective the corresponding results are written in round and squared brackets.

3-1. Multiplicity Distributions

The multiplicity distribution of the forward emitted grey particles through the present interaction with H, CNO, Em, and AgBr nuclei are presented in Fig. (1). The participation of H by one proton results in two possible channels only in the produced target fragments. Hence, the distributions in this inset have two data points only. The usual trend observed through the interactions with the other targets is the decay shape. The distributions can be approximated well by the exponential decay law of Eq. (1). The fit parameters, p_g^f and λ_g^f, are shown on the insets of Fig. (1). The decay law is presented by the smooth solid and dashed curves in Fig. (1).

$$P(N_g^f) = p_g^f e^{-\lambda_g^f N_g^f} \quad \textbf{(1)}$$

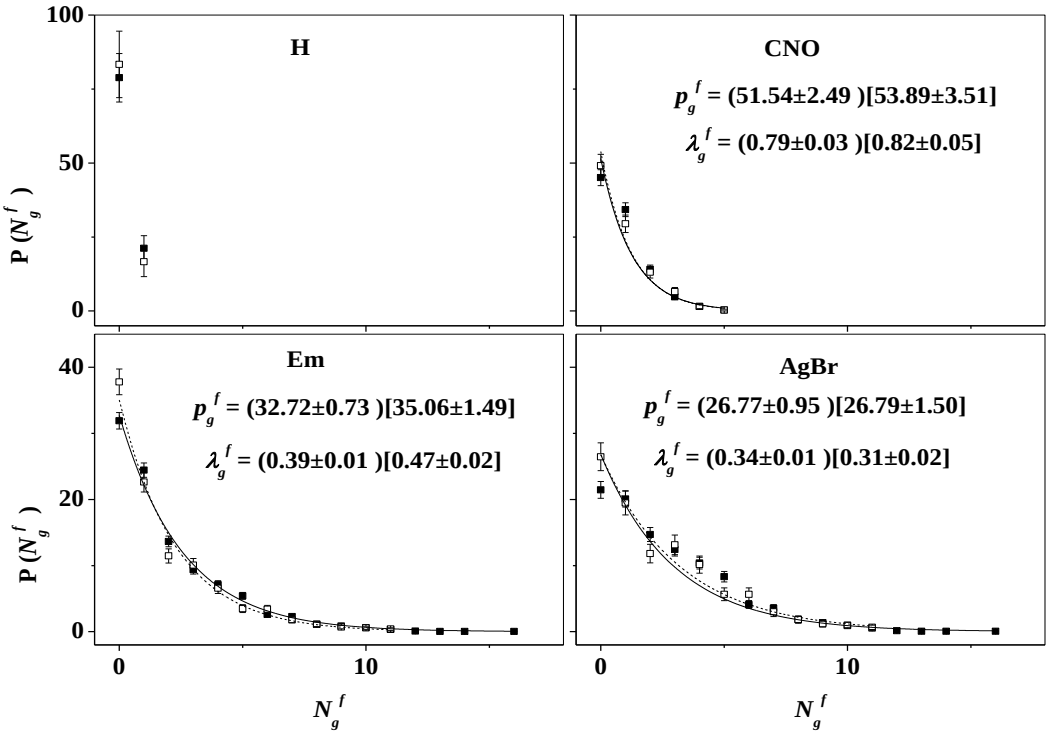

Fig. (1): The forward emitted grey particle multiplicity distributions through the present interactions, together with the fitting curves**.**

From Fig. (1), one can observe that the distributions are nearly insensitive w. r. t. the projectile size. At a certain target size, the fit parameters are the same, within experimental errors, irrespective of the projectile size. This implies a limitation in this fragmentation system w. r. t. the projectile size. This fragmentation system is investigated at ultrarelativistic regions, using two ^{16}O beams accelerated at SPS of CERN, EMU03 experiment [2]. The observed results at 60A and 200 A GeV ^{16}O interaction with emulsion nuclei [2] indicate that the decay shape distribution is characterized by λ_g^f~ 0.8, 0.4, and 0.3 for CNO, Em, and AgBr, respectively. Although the wide gap between the energy used in the present experiment and that used in Ref. [2], the fit parameters of the experimental decay law are nearly the same.

The projectile size also reveals no change in the results, where the fragmentation induced by the present ^4He and ^7Li is the same as that induced by ^{16}O [2]. Therefore Eq. (1) can be considered a universal distribution law characterizing the grey particle emitted in the FHS, regarding the NLF hypothesis w. r. t. the projectile size or energy.

In Fig. (2), the multiplicity distributions of the backward emitted grey particle through the present interaction with H, CNO, Em, and AgBr are shown. Fig. (2) exhibits a characteristic behavior as similar as that observed for the forward emitted grey particle in Fig. (1). The exponential decay law of Eq. (2) is the dominant here.

$$P(N_g^b) = p_g^b e^{-\lambda_g^b N_g^b} \quad \textbf{(2)}$$

The fit parameters, p_g^b and λ_g^b, are shown on the insets of Fig. (2). The fit parameters observed for 60A and 200A GeV ^{16}O interactions with emulsion nuclei [2] are nearly the same as those of the present experiment, where $\lambda_g^b \sim$ 2, 1, and 0.7 according to CNO, Em, and AgBr, respectively. Therefore, the NLF hypothesis is regarded also for the system of the grey particle emitted in the BHS w. r. t. the projectile size or energy. The exponential decay law of Eq. (2) can account a universality of state also, irrespective of the projectile size or energy. According to the kinematics of the collision system, the binary NN collisions and intranuclear cascading can produce the grey particle in the FHS. This mechanism is the main production source of the grey particle. The production beyond the kinematic limits in the BHS can be according to the mechanism suggested by Harris [17]. In this suggestion, each nucleon emitted in the BHS is accompanied by another one emitted in the FHS. Therefore the emission system in the BHS enhances the multiplicity of the forward emitted grey particle with a fewquantity.

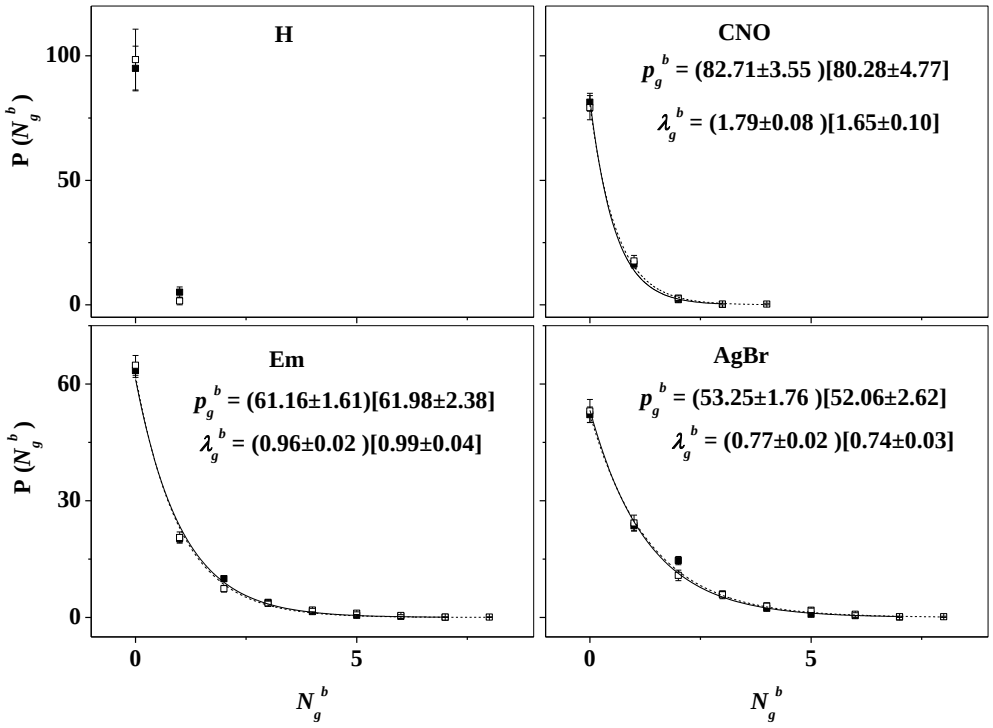

Fig. (2): The backward emitted grey particle multiplicity distributions through the present interactions, together with the fitting curves.

On the other hand, a scaling factor can be found between the forward and backward emitted grey particles multiplicities. This scaling is observed between the characteristic fit parameters where $p_g^b \sim 2\ p_g^f$ and $\lambda_g^b \sim 2.5\ \lambda_g^f$. According to this scaling, Eq. (2) can be rewritten as,

$$P\left(N_g^b\right) = 2\ p_g^f e^{-2.5\ \lambda_g^f N_g^b} \quad \textbf{(3)}$$

This scaling can imply a joint mechanism between the forward and backward emitted grey particles. Quantitatively, the enhancement of the second source to the forward emitted grey particle multiplicity is not too much to be effective in this scaling. Since the two suggested sources are originated from the formed fireball during the early stage of thermalization, hence the target participant nucleons are contributed in the two production mechanisms. The participant matter size is determined by the impact parameter. Therefore, the grey particle multiplicity itself can represent the impact parameter experimentally. Consequently, the grey particle multiplicity distributions can represent the centrality distribution. Thus the forward and backward grey particles multiplicity distributions have to decrease exponentially with the centrality in the same trend, considering the scaling factors between them.

In the framework of the NLF, the universal decay law of Eq. (3) is dependent only on the target size, A_T. Accordingly, one can express it in terms of the target mass number by correlating the fit parameters, λ_g^f, λ_g^b,

p_g^f, and$p_g^b$with A_T as shown in Fig. (3). The dependences can be approximated linearly by Eq. (4) and Eq. (5). These equations are presented in Fig. (3) by the straight line segments.

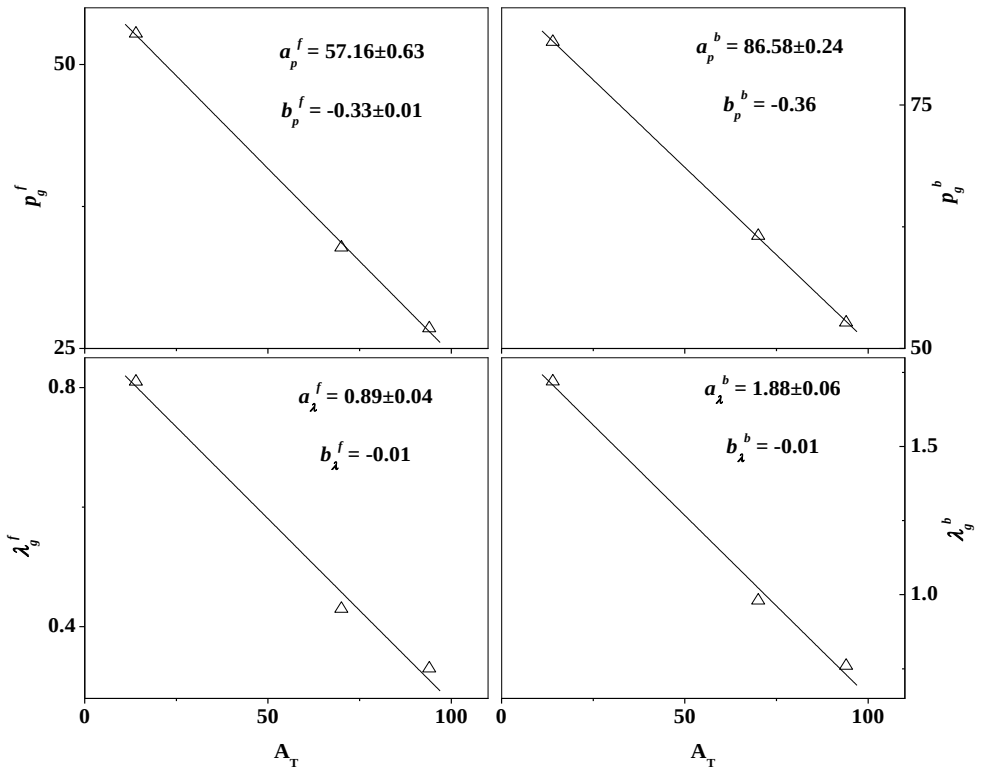

Fig. (3): The fit parameters of Eq. (3) as a function of the target mass number.

$$p_g^{f,b} = a_p^{f,b} + b_p^{f,b} A_T \quad \textbf{(4)}$$

$$\lambda_g^{f,b} = a_\lambda^{f,b} + b_\lambda^{f,b} A_T \quad \textbf{(5)}$$

The fit parameters of Eq. (4) and Eq. (5) are written on Fig. (3) insets. The slope values are nearly equal, irrespective of the emission direction in the 4–π space, where $b_p^f \sim b_p^b \sim -0.3$ and $b_\lambda^f \sim b_\lambda^b \sim -0.01$. This confirms the mentioned scaling between the forward and backward emission systems in this fragmentation region. Therefore, $a_p^b \sim 1.5 a_p^f$ and $a_\lambda^b \sim 2\, a_\lambda^f$.

3-2. Production Probabilities

The production probabilities are defined here as the statistical number of events accompanied by the grey particle emission in the FHS and BHS normalized to the total number of events. Their percentages are denoted P ($N_g^f > 0$) and P ($N_g^b > 0$), respectively. The probabilities associated with the present interactions data are illustrated against the target size in Fig. (4). From Fig. (4) one observes that the probabilities are correlated linearly with A_T. The correlations are approximated by Eq. (6). It is presented in Fig. (4) by the straight solid and dashed linear segments. The fit parameters,a_g^f,a_g^b , b_g^f, and $b_g^b$are written on the figure insets. The slope parameters, $b_g^f$and b_g^b, are nearly the same (~ 0.3), irrespective of the emission direction or the projectile size. Therefore, the production of the two emission systems has the same dependence on the target size. The intercepts are $a_g^f \sim 50$ and $a_g^b \sim 15$. Hence, the forward and backward emitted grey particles are scaled to each other by a factor = 0.3, where $a_g^b \sim 0.3 a_g^f$. Thus Eq. (6) can be rewritten as Eq. (7).

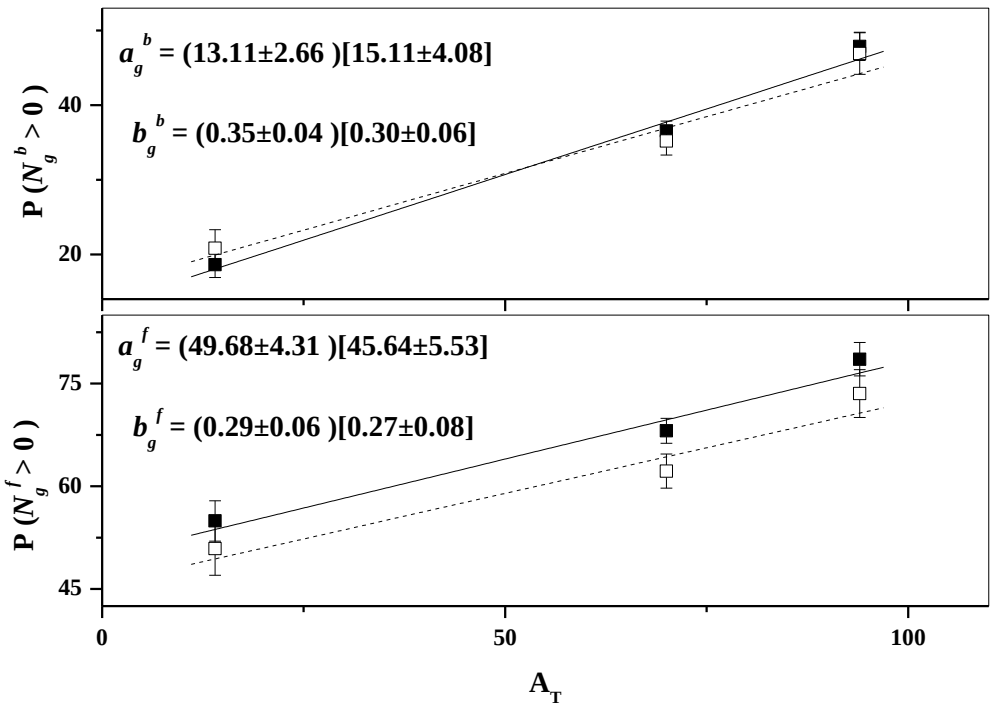

Fig. (4): The dependence of the production probabilities of the forward and backward emitted grey particles in the present interactions on the target size, together with the fitting lines.

$$P\left(N_g^{f,b} > 0\right) = a_g^{f,b} + b_g^{f,b} A_T \quad \textbf{(6)}$$

$$P\left(N_g^{f,b} > 0\right) = 50\,\alpha + 0.3\,A_T \quad \textbf{(7)}$$

where α is 1 and 0.3 in FHS and BHS, respectively. In this regime, Eq. (7) can exhibit a universal law for the grey particle production.

3-3. Average Multiplicities

The average multiplicities of the grey particles emitted in the FHS and BHS through the present interactions are correlated with the target size in Fig. (5). The correlations reveal a linear dependence on A_T for the forward and backward emitted particles. These correlations are approximated by the linear relation of Eq. (8). The fit parameters, c_g^f, c_g^b, d_g^f, and d_g^b are shown on the insets of Fig. (5) while the equation is presented by the straight solid and dashed lines. The same dependence is nearly exhibited by the forward and backward emitted particles on the target size, where the slope parameters, d_g^f and d_g^b are ~ 0.01 irrespective of the emission direction or the projectile size. The intercepts are c_g^f ~ 0.3 and c_g^b = 0.1, irrespective of the projectile size. Therefore, the forward and backward emissions are scaled to each other as c_g^b ~ 0.3 c_g^f. Basing on the observed limitation w. r. t. the projectile size and scaling between the two suggested emission systems, Eq. (8) can be rewritten in the form of Eq. (9) to exhibit a universal law for the grey particle production.

$$< N_g^{f,b} > = c_g^{f,b} + d_g^{f,b} A_T \quad \textbf{(8)}$$

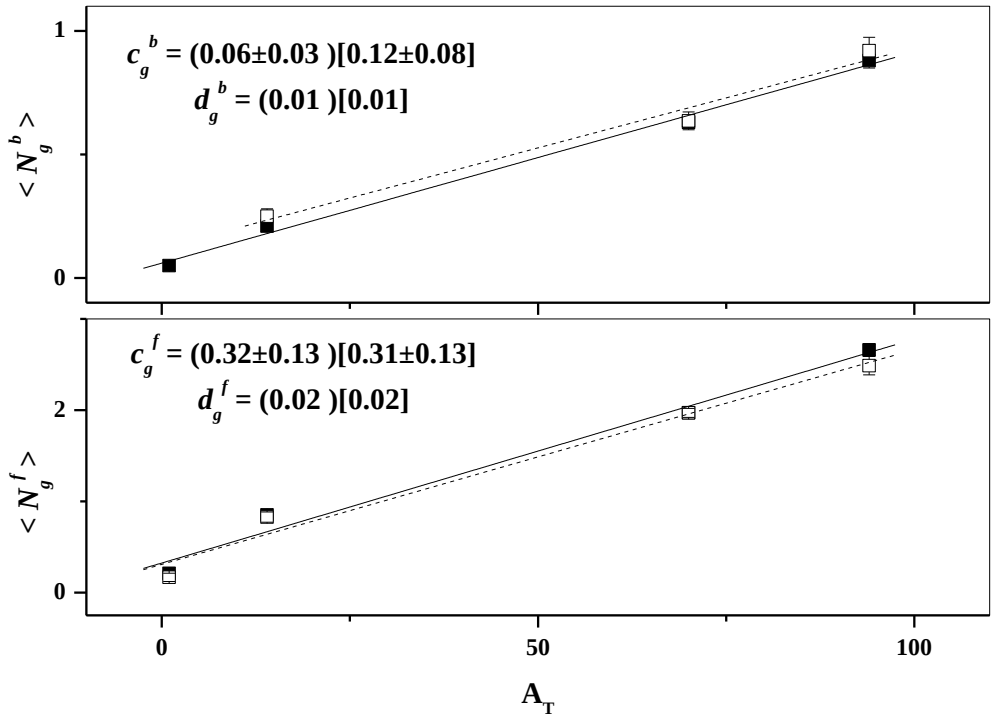

Fig. (5): The dependence of the average grey particle multiplicities in the present interactions on the target size, together with the fitting lines.

$$< N_g^{f,b} > \; = 0.3\,\beta \; + \; 0.01\,A_T \textbf{(9)}$$

where β = 1 and 0.3 for the forward and backward emissions, respectively. The same law nearly is found for 60A and 200A GeV ^{16}O interactions with emulsion nuclei [2]. This confirms the validity of the NLF hypothesis w. r. t. A_{Proj} along a wide range of E_{lab}. The universality of the grey particle production laws in the 4–π space is regarded.

Now, the asymmetry between the FHS and BHS can be determined by A_g, the so–called asymmetry parameter.

$$A_g = \frac{<N_g^f> - <N_g^b>}{<N_g^f> + <N_g^b>} \qquad \textbf{(10)}$$

The ratio, $(F/B)_g$, which is called anisotropy factor by Heckman et al [5], can measure also the production in the FHS w. r. t. the BHS.

$$(F/B)_g = <N_g^f> / <N_g^b> \qquad \textbf{(11)}$$

These two parameters are determined for the data of the present interactions and displayed in Table (3). The branching ratios of the forward and backward emitted grey particles multiplicities w. r. t. the total grey particle multiplicity, $<N_g^f> / <N_g>$ and $<N_g^b> / <N_g>$, respectively are displayed also in Table (3).

Table (3): The asymmetry parameter, anisotropy factor, and branching ratios associated with the grey particles emitted in the present interactions.

Target	A_g	$(F/B)_g$	$\langle N_g^f \rangle / \langle N_g \rangle$	$\langle N_g^b \rangle / \langle N_g \rangle$
H	(0.62) –	(4.17±1.82) –	(0.81±0.19) [1.00±0.39]	(0.19±0.01) –
CNO	(0.60) [0.54]	(4.02±0.40) [3.31±0.45]	(0.80±0.01) [0.77±0.01]	(0.20±0.02) [0.23±0.03]
Em	(0.52) [0.51]	(3.15±0.14) [2.80±0.19]	(0.76±0.03) [0.74±0.04]	(0.24) [0.26±0.02]
AgBr	(0.50) [0.46]	(3.04±0.14) [2.70±0.19]	(0.75±0.03) [0.73±0.04]	(0.25) [0.27±0.02]

From Table (3), A_g and $(F/B)_g$ are nearly 0.5 and 3, respectively irrespective of the system size. This implies that the production in the FHS is three times in the BHS. The system size is determined by both the target and projectile sizes. Since the target size is the only effective parameter in the two suggested production sources, it is reasonable that the symmetry has to change with the target size. However, the constancy is the dominant trend. This constancy is acceptable where the increase rate of the forward emitted grey particle with the target size is accompanied by the same rate of the backward emitted grey particle. The branching ratios of the forward and backward emitted grey particles w. r. t. the total grey particles emitted in the 4–π space are nearly 0.8 and 0.2, respectively irrespective of the system size or emission direction.

3-4. Multiplicity Correlations

The correlation between the forward and backward emitted grey particle multiplicities through the present interactions is shown in Fig. (6). The correlation is approximated linearly by Eq. (12).

$$< N_g^f >= e + f\ N_g^b \textbf{(12)}$$

The fit parameters, e and f, are written on Fig. (6) while Eq. (12) is presented in the figure by the solid and dashed lines. The slope and intercept parameters are nearly 1.3 and 1, respectively, irrespective of the projectile size. This value indicates that the dependence of the forward emission system on the backward one is strong. Hence, the increment rate of the forward emitted grey particle can go parallel to that of the backward emitted one.

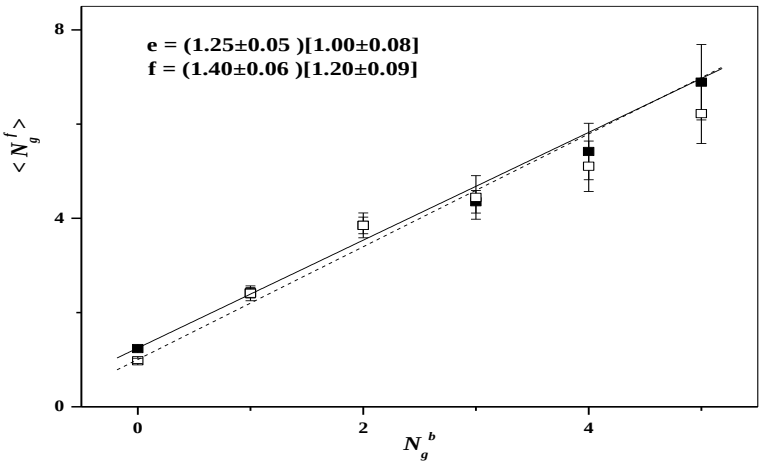

Fig. (6): The correlation between the forward and backward emitted grey particle multiplicities in the present interactions, together with the fitting lines.

The backward emitted pions are suggested to be target source particles produced through the decay of the excited target nuclei [18–22]. Accordingly, Fig. (7) shows the dependence of the forward and backward emitted grey particle multiplicities on the backward emitted pion multiplicity in the present interactions.

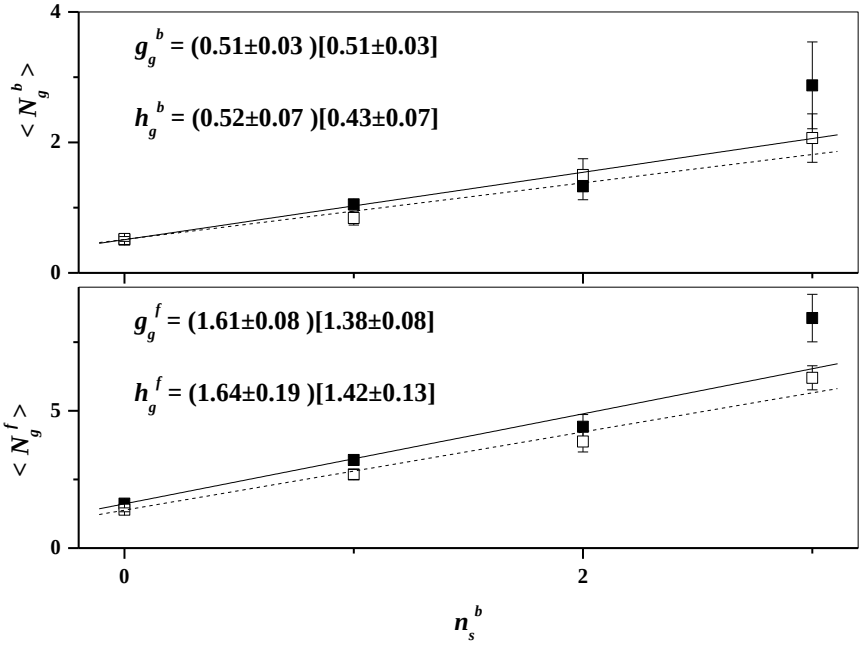

Fig. (7): The correlation between the average grey particle multiplicities and the backward emitted pion multiplicity in the present interactions, together with the fitting lines.

From Fig. (7). one observes that $<N_g^f>$ and $<N_g^b>$ depend strongly on n_s^b. The dependence is correlated by a linear relation of Eq. (13).

$$< N_g^{f,b} > = g_g^{f,b} + h_g^{f,b} n_s^b \qquad \textbf{(13)}$$

The fit parameters, g_g^f, g_g^b, h_g^f, and h_g^b are shown on the insets of Fig. (7). The correlation is presented in Fig. (7) by the straight solid and dashed lines. The dependence can not be affected by the projectile size where g_g^b ~ 0.5, g_g^f ~ 1.5, h_g^b ~ 0.5, and h_g^f ~ 1.5. Although the dependence of $< N_g^f >$ on n_s^b is stronger than that of $< N_g^b >$, one can scale the two emission systems to each other. In this scaling system Eq. (13) can be rewritten as Eq. (14).

$$< N_g^{f,b} > = \gamma\,(1 + n_s^b) \qquad \textbf{(14)}$$

where $\gamma = 0.5$ and 1.5 for BHS and FHS, respectively.

The black particle is evaporated from the spectator part of the target nucleus, as a result of its excitation. Therefore, the participant part of the target nucleus is presented by the grey particle multiplicity and the spectator part by the black particle multiplicity. Fig. (8) displays the dependence of $<N_g^f>$ and $<N_g^f>$ on N_b for the present interactions. The dependence is approximated linearly by Eq. (15) and presented by the solid and dashed lines in Fig. (8).

$$< N_g^{f,b} > = i_g^{f,b} + j_g^{f,b} N_b \qquad \textbf{(15)}$$

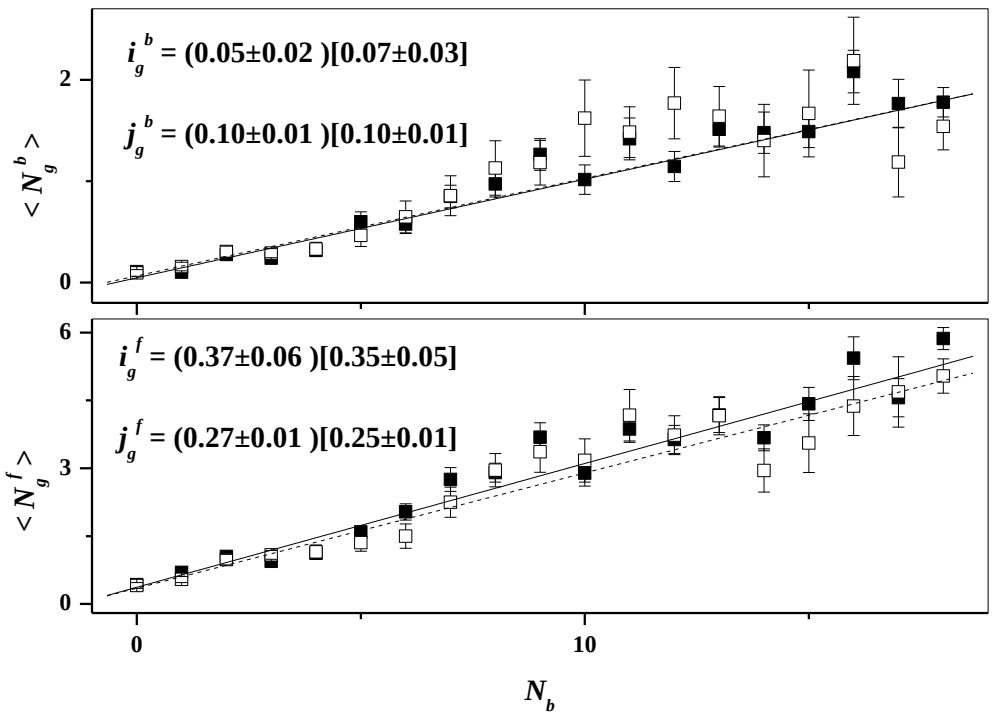

Fig. (8): The correlation between the average grey particle multiplicities and the black particle multiplicity in the present interactions, together with the fitting lines.

The fit parameters, i_g^f, i_g^b, j_g^f, and j_g^b are written on the insets of Fig. (8). They are approached as, $i_g^f \sim 0.3, i_g^b \sim 0.1, j_g^f \sim 0.3$, and $j_g^b \sim 0.1$, irrespective of the projectile size. Hence, Fig. (8) reveals that the data are insensitive to the projectile size. Although the two systems depend on the spectator target part, the slope parameters seem to be incapable of having the same dependency wieigt. However, the two systems can be scaled to each other by unifying them in Eq. (16) which is a modification of Eq. (15). The scaling factor η is 0.3 and 0.1 for the systems of the forward and backward grey particle emissions, respectively.

$$< N_g^{f,b} > = \eta\,(1 + N_b) \qquad \textbf{(16)}$$

IV. Summary And Conclusions

In conclusion, measurements of the grey particle multiplicity provide insight into the earlier stage of the target fragmentation. In the present 2.1A GeV ^{4}He and 2.2A GeV ^{7}Li interactions with emulsion nuclei, the dependence on the incident energy is not a parameter (El_{ab} ~ 2A GeV). The multiplicity is determined in terms of the target size and emission direction.

4-1. General Multiplicity Characteristics

The usual characteristic of the grey particle multiplicity distributions, either in the FHS or BHS, is the decay shape. The distributions are approximated by an exponential decay law. The fit parameters of this law depend only on the target size in a linear decrement rate. Hence the distribution law can be determined in terms of the target mass number. The production probabilities of the forward and backward emitted grey particles are approximated by a linear law relation. The average multiplicities of the forward and backward emitted grey particles are correlated with the target mass number by a linear law relation. The forward emitted grey particles are 3 times the backward emitted ones. However both of them grows in the same ratefor a constant target size. The average multiplicity of the forward emitted grey particle is correlated linearly with the backward emitted one. Linear correlationsare also exhibited for the forward and backward emitted grey particle multiplicities dependence on the backward emitted pion multiplicity and on the black particle multiplicity. The grey particle multiplicity in the FHS is always steeper than in the BHS. Kinematically in the target rest frame and according to the fireball model [8], the recoiled target nucleons through the binary NN collisions and/or intranuclear

cascading are emitted in the FHS. Hence, the intranuclear cascading is the main grey particle production source. According to Harris suggestion [17] the grey particle emitted beyond the kinematic limits in the BHS are produced from a source which is different from the forward one.

4-2. Validity of Nuclear Limiting Fragmentation

In the framework of the NLF regime, the projectile size and energy effect are examined over a widely enough range by the present light projectiles interacting at Dubna energies and ^{16}O as a heavier nucleus interacting at SPS energies [2]. The decay constants characterizing the grey particle multiplicity distributions are independent of the projectile size or energy. The production probabilities are insensitive to the projectile size. The average multiplicities are independent of the projectile size or energy. The asymmetry parameter and anisotropy ratio are nearly 0.5 and 3, respectively irrespective of the system size. The branching ratios are nearly 0.8 and 0.2 in the FHS and BHS, respectively irrespective of the system size. The approximated multiplicity correlations are independent on the projectile size. Thus the NLF is valid from Dubna energies up to SPS energies.

4-3. Scaling Assessment

A scaling behaviour is always observed between the multiplicity characteristics of the forward emitted grey particle and those of the backward emitted one. Although the two emission sources have different mechanisms, both of them originate from the formed fireball during the thermalization. Hence, the production source in the FHS works parallel to that in the BHS, considering the multiplicity amount associated with each source alone. The observed scaling can be regarded by the multiplicity distributions characteristic parameters, $p_g^b \sim 2\ p_g^f$ and $\lambda_g^b \sim 2.5\ \lambda_g^f$. The production probabilities in the FHS are scaled to those in the BHS by the parameters, $a_g^b \sim 0.3 a_g^f$. The average multiplicities in the FHS and BHS depend on the target size with a scaling system regarded by $c_g^{\,b} \sim 0.3\ c_g^{\,f}$. The multiplicity correlations of the forward and backward emitted grey particle multiplicities with the backward emitted pion multiplicity and with the black particle multiplicity can have scaling features between the emissions in the FHS and BHS.

Finally, on the basis of the NLF validity and the assessed scaling between the emission systems in the FHS and BHS a universality of state is regarded in this early stage of the target fragmentation.

Acknowledgement

This work is carried out at Mohamed El–Nadi High Energy Lab, Faculty of Science, Cairo University, Egypt. The author appreciates the guidance and advice given her by Prof. Dr. A. Abdelsalm, the head of the lab. I owe much toDr.B. M. Badawy, Dr. W. Osman and Dr. M. Fayed, the memberships of the lab, for their valuable helps. I wish to acknowledge the kind hands of Vekseler and Baldin High Energy Lab, JINR, Dubna, Russia, for supplying the photographic emulsion plates irradiated at Synchrophasotron.

References

[1]. A. Abdelsalam, N. Metwalli, S. Kamel, M. Aboullela, B. M. Badawy, and N. Abdallah, Can. J. Phys. 91, 2013,438
[2]. A. Abdelsalam, M. S. El–Nagdy, N. Rashed, B. M. Badawy, W. Osman, and M. Fayed, Can. J. Phys. 93, 2015,361
[3]. PHOBOS collaboration, Nucl. Phys. A 757, 2005,28
[4]. P. Brogueira, J. Dias de Deus, and C. Pajares, Phys. Rev. C 75, 2007,054908
[5]. H. H. Heckman, H. J. Crawford, D. E. Greiner, P. J. Lindstrom, and Lance W. Wilson, Phys. Rev. C 17, 1978,1651
[6]. A. Abdelsalam, Phys. Scr. 47, 1993,505
[7]. A. Abdelsalam, E. A. Shaat, Z. Abou–Moussa, B. M. Badawy, and Z. S. Mater, Radiation Physics and Chemistry 91, 2013,1
[8]. G. D. Westfall, J. Gosset, P. J. Johansen, A. M. Poskanzer, W. G. Meyer, H. H. Gutbrod, A. Sandoval, and R. Stock, Phys. Rev. Lett. 37, 1976,1202,
[9]. R. Stock, Phys. Rep., 1986,135, 259
[10]. C. F. Powell, F. H. Fowler, and D. H. Perkins, The Study of Elementary Particles by the Photographic Method, Pergamon Press. London, New York, Paris, Los Angles, 1958,474,
[11]. H. Barkas, Nuclear Research Emulsion, Vol. I, Technique and Theory Academic Press Inc., 1963.
[12]. V. I. Bubnov et al, Z. Phys. A 302, 1981,133
[13]. M. K. Hegab and J. Hüfner, Physics Letters B 105, 1981,103
[14]. M. K. Hegab and J. Hüfner, Nucl. Phys. A 384, 1982,353
[15]. M. Tosson, O. M. Osman, M. M. Osman, and M. K. Hegab, Z. Phys. A 347, 1994,247
[16]. Khaled Abdel–Waged, Phys. Rev. C 59, 1999,2792
[17]. J. W. Harris, Proceeding of The Workshop on Nuclear Dynamics 80, Lawrence Berkeley Laboratory, California, 17–21 March 1980.
[18]. A. Abdelsalam, B. M. Badawy, and M. Hafiz, J. Phys. G: Nucl. Part. Phys. 39, 2012,105104
[19]. A. Abdelsalam, E. A. Shaat, N. Ali–Mossa, Z. Abou–Mousa, O. M. Osman, N. Rashed, W. Osman, B. M. Badawy, and E. El–Falaky, J. Phys. G: Nucl. Part. Phys. 28, 2002,1375
[20]. M. El–Nadi, A. Abdelsalam, N. Ali–Mossa, Z. Abou–Moussa, Kh. Abdel–Waged, W. Osman, and B. M. Badawy, IL NuovoCimento A 111, 1998,1243
[21]. A. Abdelsalam, M. S. El–Nagdy, and B. M. Badawy, Can. J. Phys. 89, 2011,261
[22]. A. Abdelsalam, B. M. Badawy, and M. Hafiz, Can. J. Phys. 90, 2012,515.